Marek ADAMOWICZ[1], Patryk STRANKOWSKI[1], Jędrzej PIETRYKA[2], Janusz SZEWCZYK[2], Jarosław GUZIŃSKI[1]

Gdansk University of Technology, Faculty of Electrical and Control Engineering (1), MMB Drives Sp. z o. o. (2)

SiC-based phase-shift dual half bridge DC-DC converter as a key component of multilevel cascaded MV converters

***Abstract**. The paper describes SiC-based dual half bridge (DHB) DC-DC converter considered as a key component of high frequency isolated multilevel cascaded medium voltage converters. Two topologies of bi-directional DC-DC converters: the resonant half-bridge DC-DC converter and the phase-shift DHB converter are compared in the paper. Experimental results of SiC-based 50 kHz DHB DC-DC converter are presented in the paper.*

***Streszczenie.** W artykule przedstawiono dwukierunkową izolowaną przetwornicę półmostkową DC-DC z izolacją realizowaną za pomocą transformatora wysokiej częstotliwości jako proponowany podstawowy moduł funkcjonalny kaskadowych przekształtników średniego napięcia. Porównano dwie topologie izolowanych przetwornic półmostkowych DC-DC: rezonansową oraz ze sterowaniem przesunięciem fazowym napięć strony pierwotnej i wtórnej transformatora. Przedstawiono analizę oraz wyniki eksperymentalne przetwornicy półmostkowej DC-DC z przyrządami SiC pracującej z częstotliwością 50kHz. (**Dwukierunkowa izolowana przetwornica półmostkowa DC-DC z przyrządami z węglika krzemu jako podstawowy moduł funkcjonalny wielopoziomowych kaskadowych przekształtników SN**).*

Keywords: dual half bridge DC-DC converter, silicon carbide, cascaded multilevel medium voltage converter, zero voltage switching.
Słowa kluczowe: izolowana dwukierunkowa przetwornica półmostkowa DC-DC, węglik krzemu, kaskadowy wielopoziomowy przekształtnik średniego napięcia, przełączanie przy zerowym napięciu.

doi:10.12915/pe.2014.09.50

Introduction

The recently observed growth in heavy industry, oil and gas, mining, and traction as well, creates continued demand for medium voltage (MV) AC drives. The market situation of MV drives is driven by the rising global energy consumption and simultaneously by the increase of energy-save innovations. Nowadays trend is to replace some of low voltages drives with MV systems. In contrast to a low voltage drive, a transformer is usually not needed to reduce the voltage and to control a MV drive. From this follows, that the elimination of the line frequency input transformer results in significant weight and size reduction of the drive system, therefore it is an important advantage of MV solutions.

The new generation of four quadrant MV converters with isolation, realized at high frequency (Fig. 1a) [1 - 3], are now entering the phase of pre-production testing prior to their commercial. They are built of a connected cascade of AC-DC-DC-AC modules including H-bridge inverters and high frequency transformers, ensuring galvanic isolation. In contrast to conventional industrial drives powered from AC mains, modern traction drives feed from DC traction network need isolated DC-DC-AC converter. The first high frequency isolated DC-DC-AC converters made from 3.3 kV and 6 kV IGBTs have been recently developed, commissioned and successfully installed in locomotives [4, 5].

The research works concerning bidirectional MV power converters are currently focused on improving efficiency and reliability, increasing power density and simplifying design, and thereby increasing their competitiveness in comparison with LV systems equipped with line frequency transformers. A promising strategy to achieve these objectives is a Power Electronics Building Block (PEBB) approach [6, 7]. PEBBs are expected to be key components of the future high power MV converters. The key component of both AC-DC-DC-AC and DC-DC-AC modules is the bidirectional isolated DC-DC converter, which can be designed as resonant half bridge DC-DC converter [4, 5] or as phase-shift dual half bridge (DHB) DC-DC topology [9, 10].The half bridge DC-DC converters consist of only four switches. This fact results in a reduction of on-state losses, compared to dual active bridge (DAB) DC-DC converters comprising two fully controlled H-type transistor bridges [2, 3, 10, 12].

The main advantage of DAB converters over DHB converters is the existence of additional degrees of freedom. That can be applied in the control algorithm, e.g. by implementing zero vectors and variable duty cycle in the PWM voltage generation algorithm. However the lower losses of DHB converter and easier implementation of zero voltage switching (ZVS) technique, in a whole operating range, makes the half bridge DC-DC converters very attractive for multilevel cascaded MV converters [4, 5, 9]. Additionally, at the same value of DC-link voltage, the half bridge DC-DC converters characterize a twice smaller voltage across transformer windings which makes them less problematic from an insulation issues. The detailed comparison of the operational conditions of DAB and DHB converters can be found in [9].

For the foreseeable future it can be observed that conventional silicon (Si) systems based on IGBT transistors will dominate in high power multilevel converters [13]. In the case of MV adjustable speed drives the concept of cascading converter cells based on 1.7 kV, 3.3 kV or 6 kV IGBTs is usually considered. On the one hand the selection of IGBTs with high enough blocking voltage provides the lower number of cascading converter cells per phase, but on the other hand it causes an unfavorable reduction in switching frequency and significant increase in size of magnetic circuits and deterioration in the quality of the generated voltage.

Progress in SiC devices (>1 kV SiC MOSFETs, SiC JFETs and SiC Schottky diodes) enables to push-forward the MV voltage source converter (VSC) technology [7]. A SiC field effect transistors can replace Si IGBTs of much higher rated current. Currently 600V 150A and 1200V 100A SiC MOSFETs are available on the market. The Implementation of SiC semiconductor switches in bidirectional DC-DC converters provides an opportunity to increase the working frequency of high-power converters, decrease the system size and to eliminate an acoustic noise as well. Moreover the increase in voltage levels, by cascading 1.2 kV SiC-based converter cells, provides a smaller size of line side filters. This results in an IGBT-based system with a few output voltage steps and much lower switching frequency [13].

Based on the results obtained in [9], for Si MOSFET-based DHB converter for 7.2kV/0.4kV with solid state transformer, the aim of investigations discussed in present paper is to get the knowledge on high switching phase-shift DHB converter based on SiC devices regarding future application in a modular multilevel cascaded MV converter. Zero voltage switching technique is discussed as a way to provide low switching losses of the converter. Similarly to [9], a planar power transformer with ultra-low leakage inductance is used in the experimental setup of developed SiC-based DHB converter.

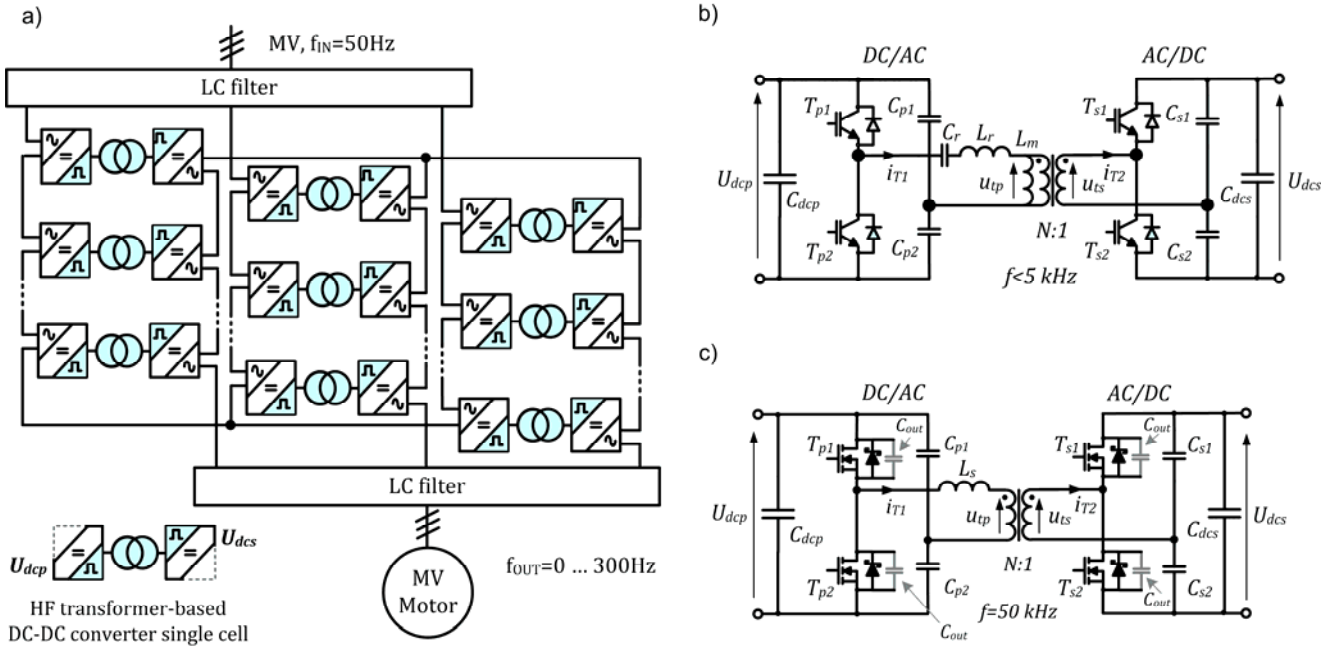

Fig. 1. MV motor drive system utilizing multilevel cascaded MV converter (a), Si-based resonant half bridge DC-DC converter with four quadrant operation (b), and SiC-based phase-shift dual half bridge DC-DC converter considered in the paper (c)

The comparison of resonant half bridge and phase-shift dual-half-bridge(DHB) DC-DC converters

The Si-based resonant half bridge DC-DC converter and SiC-based DHB DC-DC converter under consideration are shown in Fig.1(b) and Fig. 1(c). The variables in Fig. 1 are as follows: U_{dcp} – primary side DC voltage, U_{dcs} –secondary side DC voltage, N – transformer turns ratio, $C_{p1,2}$ and $C_{s1,2}$ – primary and secondary side voltage splitting capacitors, C_{dp}, C_{ds} – primary and secondary side DC-link capacitors, C_r, L_r – capacitor and inductor of the resonant circuit of resonant DC-DC converter, L_s – sum of transformer leakage inductance L_σ and commutation inductor L_{s1} for energy storage during power conversion in DHB DC-DC converter.

LLC resonant converters have been developed to overcome several limitations of classical series resonant converters, which were incapable of regulating under unloaded condition. The LLC resonant half bridge converter shown in Fig. 1(b) has the same configuration as the 3.3 kV/6.5 kV 1.75 kHz IGBT based resonant half bridge DC/DC converter, used in power electronic traction transformer (PETT) of ABB [4] for 15 kV, 16⅔ Hz railway grid applications. LLC resonant half bridge converter described in [4] operates with 1.7 kHz switching frequency and 50% duty cycle PWM. The difference between primary voltage U_{dcp} and secondary voltage U_{dcs} applied to a resonant L_r–L_m–C_r circuit from Fig. 1(b) generates resonant current which is sinusoidal with the resonant frequency. The resonant capacitor C_r connected in series with primary or secondary windings makes automatic flux balancing and high resonant frequency with the resonant inductance. Moreover, it protects the transformer core from saturation. LLC resonant converter has two resonant frequencies f_{r1} and f_{r2} which both play important role in converter operation [1, 5]:

$$f_{r1} = \frac{1}{2\pi\sqrt{L_r C_r}} \tag{1}$$

$$f_{r2} = \frac{1}{2\pi\sqrt{(L_m + L_r)C_r}} \tag{2}$$

The resonant circuit, consisting of L_r, C_r and transformer magnetizing inductance L_m, is designed that the resonant frequency f_{r1} is identically to the switching frequency f_s of the DC-DC converter. Depending on the power flow, either primary or secondary side of the LLC resonant converter is PWM controlled, while the other side acts like a diode rectifier, respectively [1]. Therefore in the motoring mode of the PETT secondary side IGBTs are in the off-state and only anti-parallel free-wheeling diodes conduct [4]. When the switching frequency is lower than the resonant frequency, the resonant half bridge DC-DC converter from Fig. 1(b) operates in discontinuous current mode.

The proposed phase-shift DHB DC-DC converter shown in Fig. 1(c) consists of two SiC-based phase-legs [7] and a 50 kHz planar power transformer. Planar magnetic components are beneficial and cost effective for conversion frequencies above 20 kHz, especially in large production quantities [15].

The SiC-based transistors and two capacitor-based voltage dividers on each side of the transformer are used to generate a square-wave voltages applied to the primary and secondary side of the transformer. The power flow is determined by the phase difference φ between the primary- and secondary-pole voltages [8, 9]:

(3) $$P_{out} = \frac{N \cdot (U_{dcp}/2) \cdot (U_{dcs}/2)}{2\pi^2 f_s L_s} \cdot \varphi(\pi - |\varphi|)$$

where: $-\pi/2 < \varphi < \pi/2$

The value of the capacitors C_{p1}, C_{p2} and C_{s1}, C_{s2} are selected large enough to obtain fixed voltages across the capacitors during each switching period. From (4) it can be seen that the output current I_{ds} of the DHB converter is independent from the secondary voltage U_{dcs} [9], so that DHB converter fed electric drive behaves like a current source.

(4) $$I_{out} = \frac{P_{out}}{U_{dcs}} = \frac{N \cdot U_{dcp}}{8\pi^2 f_s L_s} \cdot \varphi(\pi - |\varphi|)$$

As it has been stated in [9], a multiple DHB converters can be directly connected in parallel to extend the power rating with no necessity of additional superior control. This is an important advantage in the case of application in high-power MV drives.

In Table 1 the advantages and disadvantages of the resonant half bridge DC-DC and DHB topologies are indicated.

Table 1. Advantages and disadvantages of the resonant half bridge DC-DC and phase-shift DHB topology

Resonant half bridge DC-DC converter	Phase-shift DHB converter
Advantages	
• lower switch count than in full bridge converters, • wide output regulation range, • reduction of switching losses on the primary side through zero voltage switching (ZVS) over the entire load range, • lack of a DC current through a transformer, • low turn-off current controlled by the design, • load independent operation at resonant frequency.	• lower switch count than in full bridge converters, • wide output regulation range, • reduction of switching losses on the primary side through zero voltage switching (ZVS) over the entire load range, • smaller transformer core loss than in dual active bridge converter, • simple control of the converter based on phase shift modulation, • asymmetric duty cycle control for elimination of the voltage unbalance in the secondary side of DHB.
Disadvantages	
• large ratio of the two resonant inductors (transformer magnetizing inductance and L_r) is required to reduce the IGBT turn-off currents which results in a reduced range for the output voltage control, • open loop control typically used, • closed loop control requires wide variation of switching frequency, which can severely compromise the efficiency of the converter, • the duty cycle of generated transformer voltages has to be controlled carefully to avoid the saturation, • switching frequency lower than resonant frequency causes operation in discontinuous current mode.	• high ripple current of the splitting capacitors of the voltage divider(However it should be pointed that several types capacitors, e.g. metallized propylene, and designed in self-healing film/foil technology, operating with DC voltages up to few kV, and rms currents up to 1kA are available on the market [16]), • unequal load of semiconductor devices, • possible unbalance in the secondary side of DHB.

ZVS operation of SiC-based DHB converter

The energy circulating in the converter circuit, influences the switching losses of the converter. During hard switching operation the energy stored in the intrinsic output capacitance of each individual switch is dissipated in the channel, decreasing the whole efficiency of converter. The DHB converter discussed in the paper utilizes zero voltage switching (ZVS) technique to achieve low switching losses. Low power Si MOSFET-based resonant DC-DC converters can utilize intrinsic output capacitance of the transistors to maintain ZVS operation, but in most cases an external output capacitance is used to reduce the turn-off loss by converting the load current to the energy stored in external capacitance.

During the operation, the commutation inductor L_s of DHB converter stores a portion of energy E_c which subsequently circulates in the converter circuit [16]. The circulating energy E_c is employed to discharge the output capacitance C_{cout} of individual switches (Fig. 1(c)). ZVS operation of DHB converter is maintained, if the circulating energy is no less than the total ZVS threshold energy, i.e. no less than total energy stored in the output capacitance C_{out}. The circulating energy E_c increases with square of phase shift and thus with output power. This is inversely proportional to square of switching frequency and commutation inductance L_s [9]:

(5) $$E_c = \frac{\varphi \cdot P_{out}}{2 \cdot f_s \cdot (\pi - |\varphi|)} = \frac{N \cdot U_{dcp} \cdot U_{dcs} \cdot \varphi^2}{16 \cdot \pi^2 f_s^2 L_s} .$$

The energy E_L stored in commutation inductor L_s during single transition is equal to the half of the total circulating energy:

(6) $$E_L = \frac{E_c}{2}$$

It was reported in [6], that with insufficient E_c the ZVS operation of Si-based DHB converter is lost. On the other hand the excessive circulating energy causes additional conduction losses.

Furthermore, in isolated dc-dc converters, the dead-time has a significant influence on ZVS performance and converter efficiency in the presence of varying loads [17] – [19]. A minimum commutation current is required to ensure the resonant transition within the dead-time interval. On the one hand, if the dead-time is too short, the transistor may be turned on before the resonance is done, by causing additional losses. On the other hand, a too long dead-time may cause a re-resonance phenomena at light loads [19]. The minimum commutation current required to complete the resonant transition of isolated DC-DC converter may be calculated in the control algorithm and dead-time interval can be derived according to the optimal values of duty cycle and the phase-shift [18].

Design example of 20 kW DHB converter for 3.3 kV 300 kVA multilevel cascaded converter

The number of cascade connections N_C of the multilevel cascaded MV converter from Fig. 1a, depends on the DC-

link voltage U_{dcp} in each converter cell, which in turn depends on the maximum permitted blocking voltage of used power switches. For 1200 V SiC MOSFETs and 1200V SiC JFETs, considered in the paper, N_C =5 and U_{dcp} = 750 V. If the rated power of the 3.3 kV multilevel cascaded converter is 300 kVA with N_C =5, the rated power of the single DHB converter cell is 20 kW. To achieve a higher current rating needed in modular high power converters a parallel connection of two SiC MOSFETs / two SiC JFETs in each switch is proposed. The current and voltage ratings of the used *normally-off* SiC devices are shown in Table 2.

Table 2. Ratings of the switching devices

	2*SiC JFET	**2*SiC MOSFET**
Voltage rating	V_{ds} =1200V	V_{ds} =1200V
Current rating	I_d =2*40A @100°C	I_d=2*42A @25°C
On-state resistance	$R_{ds(on)max}$ =0.035 Ω	$R_{ds(on)max}$ =0.05Ω

For galvanic isolation a 50 kHz transformer containing UIIU/93/245/30 core made of N87 material is used. Table 3 shows parameters of the designed 20 kW DHB converter.

Table 3. Parameters of the 20 kW, 50 kHz DHB converter

Input voltage, output voltage	U_{dcp}, U_{dcs}	750 V
Rated power	P_{out}	20 kW
Operating frequency	f_s	50 kHz
Transformer input/output voltage	u_{tp}, u_{ts}	375 V
Transformer turns ratio	N	18:18
Transformer core material		N87
Transformer leakage inductance	L_σ	2μH
Maximum AC flux density	B_{max}	0.25 T
Cross-section area	A_c	8.46 cm^2
Commutation inductor	L_{s1}	10 μH
Snubber capacitors	C_{out}	3 nF
Splitting Capacitors	C_{p1},…C_{s2}	30 μF

Connecting a snubber capacitor C_{out} in parallel to each *normally-off* switch in Fig. 1b realizes ZVS operation. Ceramic capacitors with 3nF and 2kV have been selected for this.

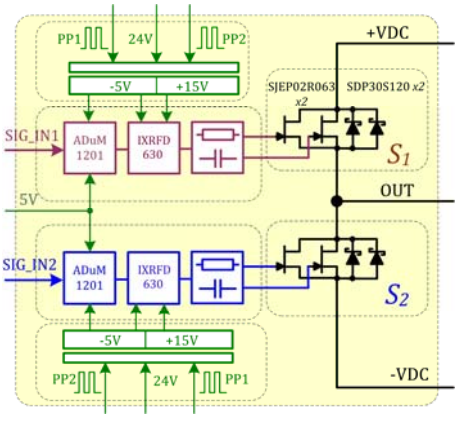

Fig. 2. Circuit scheme of the proposed IXRFD630-based universal gate drivers for precise generation of gate signals.

Automatic control of transistors dead-times needed for extending ZVS range requires precise generation of gate signals with very high bandwidth. The proposed gate driving circuit [7] is realized using low impedance IXYS gate driver IXRFD630 (formerly DEIC 420) and digital isolator ADuM1201. The used low impedance driver features a peak current capability of over 20 A and voltage rise and fall times less than 4 ns. Hence it is capable to precise control of dead-time length as well as to charge and discharge the input gate and 'Miller' capacitances of the controlled transistors with times less than 10ns. The paralleling of switching devices increases the current path length of the gate circuits and may decrease the available peak gate current. The proposed universal gate driver enables to drive up to four SiC MOSFETs operated in parallel and up to three SiC JFETs having turn on peak current of 5.5 A each and turn on time of less than 100ns. The converter leg with two SiC JFET-based 80A, 1200V switches S1 and S2 and proposed IXRFD630-based gate driving circuits with appropriate isolated and non-isolated power supply circuits is shown in Fig. 2. The characteristic voltage and current waveforms of the proposed gate driving circuit are shown in Fig. 3.

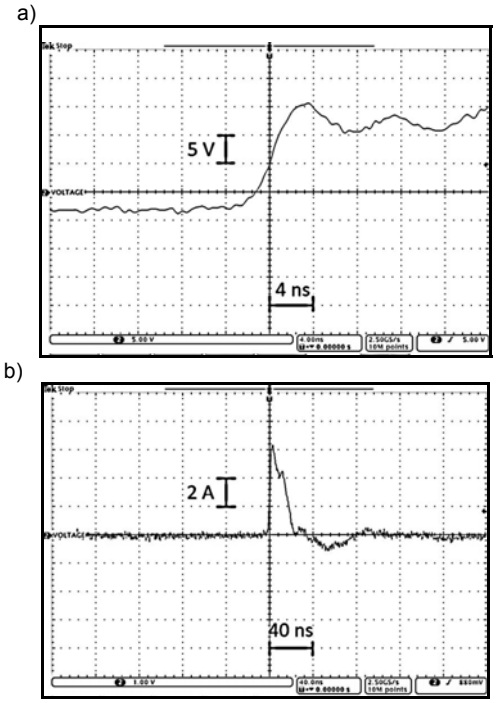

Fig. 3. Voltage (a) and current (b) signals of the proposed high speed universal gate driver during 'turn on' operation.

Simulation results

Simulation model of the proposed DHB converter from Fig. 1c was prepared in PSIM simulation software with the use of parameters from Table 2 and Table 3. Simulation tests were done for full load, P_{out} =20 kW , light load, P_{out} =2 kW and for DC-link voltage U_{dcp1} =750 V. At the performed tests, the attention was paid at the distribution of the voltages of the splitting capacitors C_{p1}, C_{p2} and C_{s1}, C_{s2}. The ac-components in voltages on splitting capacitors as well the magnitudes of charging and discharging currents were also examined. Fig. 4 shows the characteristic waveforms of investigated DHB converter at full load, with phase shift φ =0.36 rad. Currents and voltages waveforms at light load, P_{out} =2 kW and phase shift φ =0.03 rad, are shown in Fig. 5. It can be seen, that with the used value of commutation inductance L_{s1} =10μH, the compromise between maintaining of limited circulating energy and ensuring the smallest fluctuation of splitting capacitors voltages was reached.

Dynamic characteristics recorded during primary side switch T_{p2} *turn-on* are shown in Fig. 6. Figures 6a and 6b show the T_{p2} switching waveforms at full load and light load with fixed dead-time and Fig. 6c shows the switching transients with automatic dead-time control.

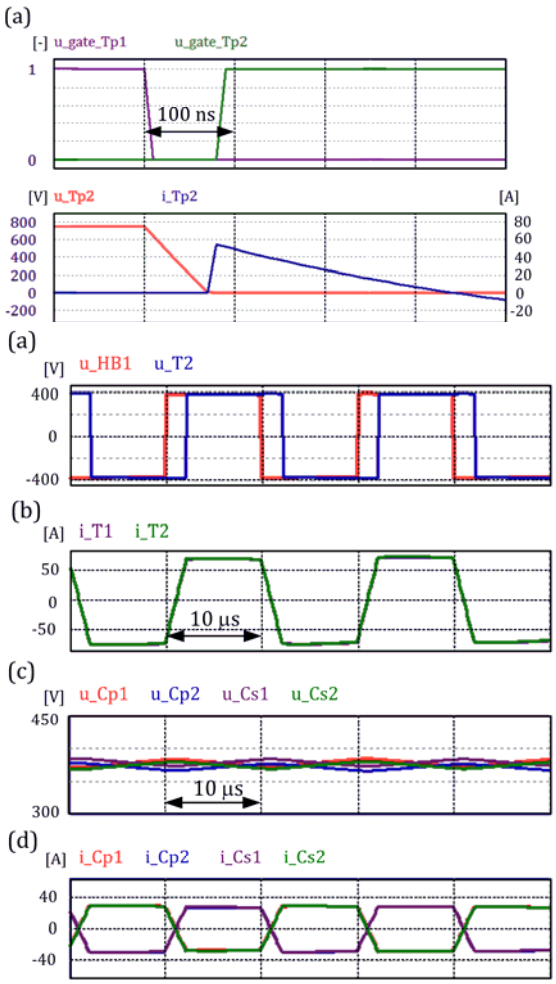

Fig. 4. Characteristic waveforms of investigated DHB converter operating at full load, Pout=20 kW and phase shift φ =0.36 rad: primary and secondary half bridge voltages u_{HB1}, u_{T2} (a); primary and secondary transformer currents i_{T1}, i_{T2} (b); splitting capacitors voltages u_{Cp1}, u_{Cp2} and u_{Cs1}, u_{Cs2} (c); charging and discharging currents of splitting capacitors i_{Cp1}, i_{Cp2} and i_{Cs1}, i_{Cs2} (d).

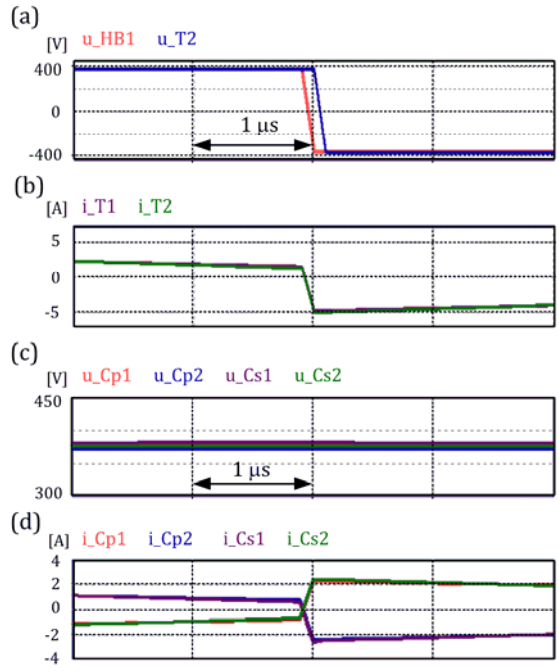

Fig. 5. Characteristic waveforms of proposed DHB converter operating at light load, Pout=2 kW, and phase shift φ =0.03 rad: half bridge voltages u_{HB1}, u_{T2} (a); transformer currents i_{T1}, i_{T2} (b); splitting capacitors voltages u_{Cp1}, u_{Cp2} and u_{Cs1}, u_{Cs2} (c); charging and discharging currents of splitting capacitors i_{Cp1}, i_{Cp2} and i_{Cs1}, i_{Cs2} (d).

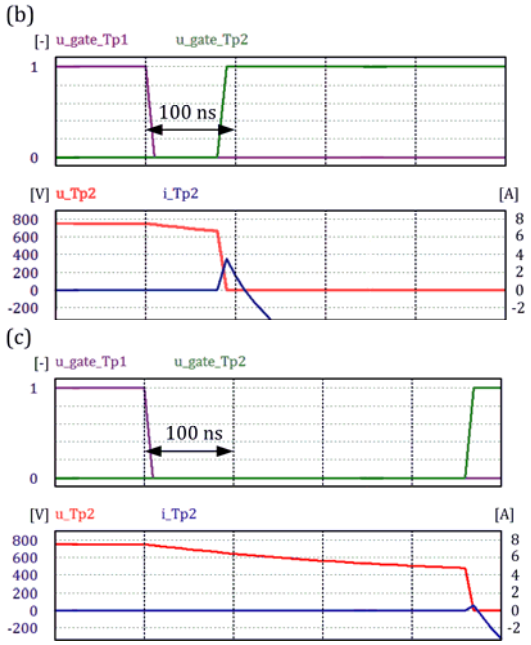

Fig. 6. Simulated transients during primary side switch T_{p2} *turn-on* (gate signals of T_{p1} and T_{p2} on the top): ZVS operation at full load with commutation inductor peak current of 69 A and fixed dead-time of 100 ns (a); lack of ZVS condition during light load operation with inductor peak current i_{Ls} =7A and fixed dead-time of 100 ns (b); almost ZVS operation at light load and dead-time adjusted to value of commutation inductor current (c).

It can be seen from Fig. 6c that the application of automatic control of dead-times extends the ZVS operation range of the proposed DHB converter.

Experimental tests of 2kW DHB converter model

Experimental results obtained from a 2 kW SiC-based DC-DC converter are given in this chapter to validate the analysis and practical feasibility of the proposed system. The laboratory model of the bidirectional phase-shift SiC-based DHB using CMF20120D SiC MOSFETs, SJEP02R063 SiC JFETs and 3kW 14:12 power planar transformer with 47µH commutating inductor was developed. Table 4 presents other parameters of the developed laboratory model. The input and output voltage of the investigated SiC-based DHB converter are chosen as 415 V and 230 V respectively. The current and voltage waveforms were observed and recorded using LeCroy WaveSurfer 424 200MHz 2GS/s oscilloscope equipped with Tektronix TCPA 300 and TCP 305 50A current probes and TesTEC TT-SI 9110 100MHz voltage probes. SiC Schottky diodes of C2D20120D Series have been used with SiC MOSFETs and SDP30S120 SiC Schottky diodes with SiC JFETs. That is according to recommendations given in [14]. The developed laboratory setup is shown in Fig. 7.

The investigated DHB converter is feed from 3x400V 50Hz autotransformer via diode rectifier.

The 500 µF capacitors are used in primary side and secondary side DC-links. The additional wires connected to SiC devices visible in Fig. 7c and Fig. 7d are used only for measurements. Figures 8 to 12 presents characteristic waveforms of the developed laboratory model of 50 kHz SiC-based DHB converter. Fig. 8 shows steady-state waveforms of the drain-source voltages of primary side switch T_{p2} and secondary side switch T_{s2} and commutating

inductor current i_{T1} during DHB converter operation with phase shift φ =1.26 rad (Pout=1.5 kW). The performance of the proposed ultrafast universal gate driver is shown in Fig. 9.

Table 4. Parameters of the 2 kW DHB converter laboratory model

Input voltage	U_{dcp}	415 V
Output voltage	U_{dcs}	230 V
Transformer Type	*HIMAG 134403 Series*	
Transformer rated power	P_{out}	2 kW
Operating frequency	f_s	50 kHz
Transformer input/output voltage	u_{tp}, u_{ts}	207V, 115 V
Transformer turns ratio	N	14:12
Transformer core material		3F3
Transformer leakage inductance	L_σ	1μH
Commutation inductor - 20 turns	L_{s1}	47 μH
Splitting Capacitors MKP4 1100V	C_{p1},…C_{s2}	10 μF

a)

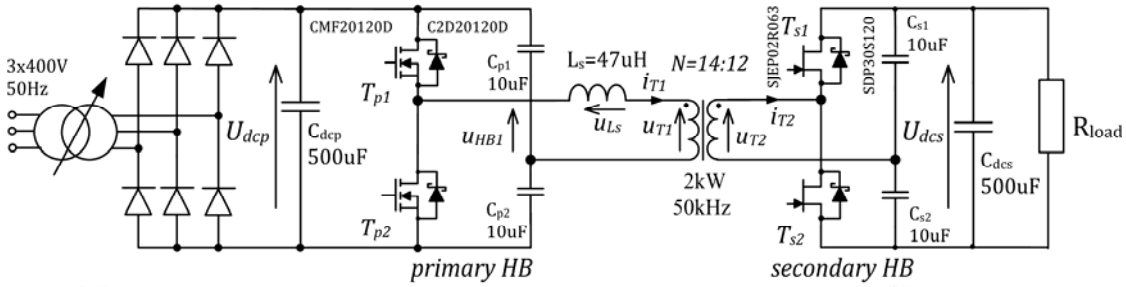

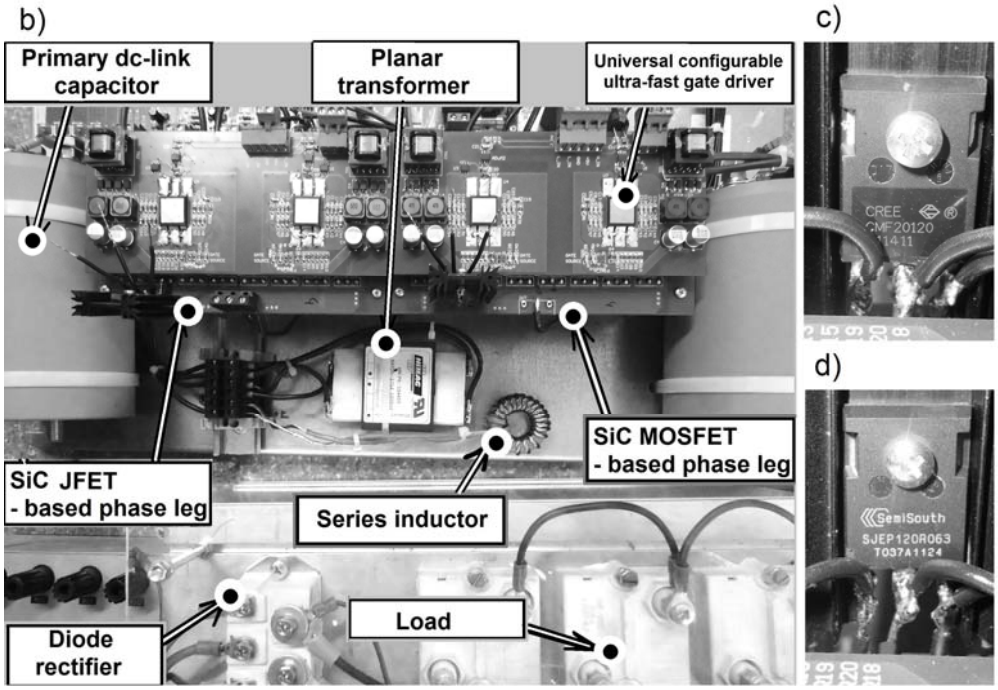

Fig. 7. The laboratory setup with proposed 50 kHz SiC-based DHB converter with 2 kW power planar transformer: circuit schematic (a); the overall view (b); investigated SiC MOSFET (c) and SiC JFET(d).

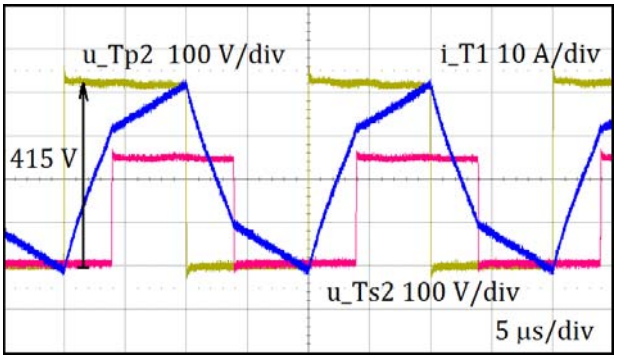

Fig. 8. Primary side switch T_{p2} and secondary side switch T_{s2} drain-source voltages and commutating inductor current i_{T1} with phase shift φ =1.26 rad (P_{out}=1.5 kW)

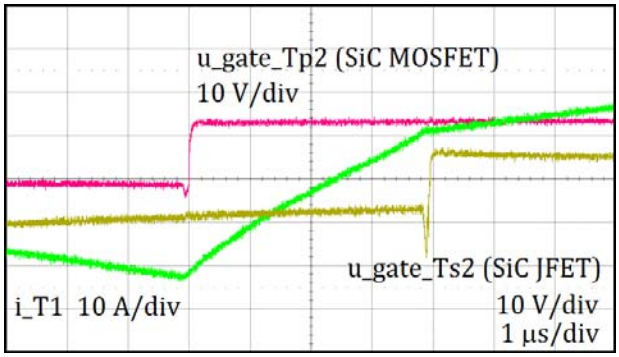

Fig. 9. Performance of proposed ultrafast universal gate driver: generated gate voltages of SiC MOSFET (T_{p2}) and SiC JFET (T_{s2}). In the background current i_{T1}.

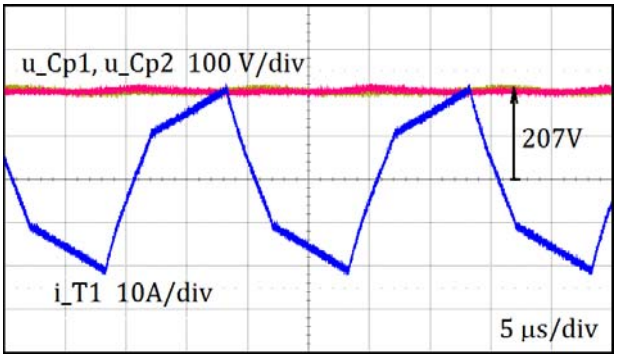

Fig. 10. Voltages u_{Cp1}, u_{Cp2} of the primary side splitting capacitors. In the background commutation inductor current i_{T1}.

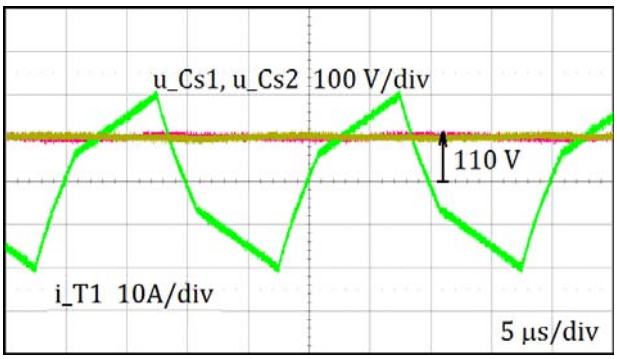

Fig. 11. Voltages u_{Cs1}, u_{Cs2} of the secondary side splitting capacitors. In the background commutation inductor current i_{T1}.

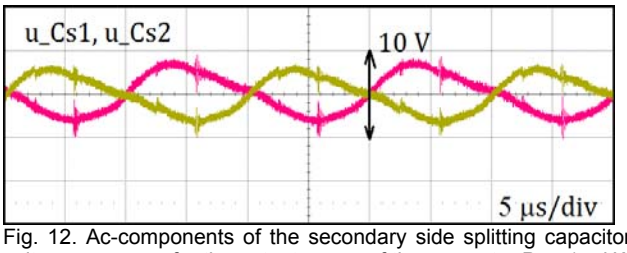

Fig. 12. Ac-components of the secondary side splitting capacitors voltages u_{Cp1}, u_{Cp2} for the output power of the converter P_{out}=1.5 kW.

The distribution of the voltages of the primary side and secondary side splitting capacitors is shown in Fig. 10 and Fig. 11. The oscillations in secondary side splitting capacitors voltages can be seen in Fig. 12. These oscillations depend on the load and for higher loads should be controlled by the control of commutation inductor current i_{T1} , to improve the converter performance. These oscillations could be minimized at the design stage by proper selection of DHB converter parameters.

Conclusions

In this paper the analysis of a bidirectional dual half bridge DC-DC converter with SiC devices operating at 50 kHz switching frequency was presented. The intended use of this converter is in a module of MV converters. Presented design example of 20 kW DHB converter shows the possibility of using the system in the 300 kVA multilevel cascaded converter for 3.3 kV induction motor drives. The converter circuit was implemented with SiC MOSFET, and SiC JFET transistors, and SiC Shottky diodes. An ultrafast universal gate driver for SiC MOSFETs and SiC JFETs which enable precise generation of gate signals with controlled dead-time length was proposed. The automatic control of transistors dead-times enables to extend the range of ZVS operation of DHB converter and to improve its efficiency. Due to the four layer PCB-layout design, the line length and simultaneously the parasitic parameters of the SiC transistor driver circuit were significantly minimized. The developed universal, configurable gate driver circuit allows to implement different types of SiC transistors at the laboratory model. The commutation inductor connected in series with high frequency transformer plays a major role in the investigated DHB converter. The increase of commutation inductance enables the minimization of the oscillations in voltages of the splitting capacitors but in the other hand causes the decreases the maximum allowable output power The analysis and simulation results was successfully verified on laboratory model of 50 kHz SiC-based DHB converter with a 2 kW power planar transformer

Acknowledgement

Projekt został sfinansowany ze środków Narodowego Centrum Nauki przyznanych na podstawie decyzji numer DEC-2013/09/B/ST7/01642.

REFERENCES

[1] Schibli N., Symmetrical multilevel converters with two quadrant DC-DC feeding, *PhD Thesis*, EPFL Lausanne, 2000.

[2] Innoue S., Akagi H., A bidirectional isolated DC–DC converteras a core circuit of the next-generation medium-voltage power conversion system, *IEEE Transaction on Power Electronics*, Vol. 22, (2007), No 2, 535-542.

[3] Jiang D., Xue J., Kao M. H., Fred Wang, High Density Modular Multilevel Cascade Converter for Medium-Voltage Motor Drive, *IEEE Electric Ship Technologies Symposium ESTS*, (2011), 482-485.

[4] Dujic D., Chuanhong Zhao, Mester A., Steinke J.K., Weiss M., Lewdeni-Schmid S., Chaudhuri T., Stefanutti, P., Power electronic traction transformer-medium voltage prototype, *IEEE Transactions on Power Electronics*, Vol. 99, (2013), No 99, 1 - 11.

[5] Dujic D., Steinke G.K., Bellini M., Rahimo M., Storasta L., Steinke J.K., Characterization of 6.5 kV IGBTs for high-power medium-frequency soft-switched applications, *IEEE Transactions on Power Electronics*, Vol. 29, (2014), No 2, 906 - 919.

[6] Ericsen T., Khersonsky Y., Schugart P., Steimer P., PEBB – power electronics building blocks, from concept to reality, Proc. *3rd IET Conference on Power Electronics, Machines and Drives*, (2006), 12-16.

[7] Adamowicz M., Strzelecki R., Krzeminski Z, Hybrid high-frequency-SiC and line-frequency-Si based PEBB for MV modular power converters, *Proc. 38th Annual Conference on IEEE Industrial Electronics Society IECON*, (2012), 5197-5202.

[8] Peng F. Z., Li H., Su G. J., Lawler J.S., A New ZVS Bidirectional DC–DC Converter for Fuel Cell and Battery Application, *IEEE Transactions on Power Electronics*, Vol. 19 (2004), No 1, 54 – 65.

[9] Fan H., Li H., High-frequency transformer isolated bidirectional DC–DC converter modules with high efficiency over wide load range for 20 kVA solid-state transformer, *IEEE Transaction on Power Electronics*, Vol. 26, (2011), No 12, 3599 – 3608.

[10] Gangyao Wang, Huang A., Chushan Li, ZVS range extension of 10 A 15 kV SiC MOSFET based 20 kW dual active half bridge (DHB) DC-DC converter, *Proc. IEEE Energy Conversion Congress and Exposition ECCE*, (2012), 1533-1539.

[11] YanhuiXie, Jing Sun, Freudenberg, J.S., Power flow characterization of bidirectional galvanically isolated high-power DC/DC converter over a wide operating range, *IEEE Transactions on Power Electronics*, Vol. 25, (2010), No 1, 54 – 66.

[12] Hua Bai, Ziling Nie, Mi, C.C., Experimental comparison of traditional phase-shift, dual-phase-shift, and model-based control of isolated bidirectional DC–DC converters, *IEEE Transaction on Power Electronics*, Vol. 25, (2010), n. 6, 1444 – 1449.

[13] Huber J., Kolar J. W., Optimum number of cascaded cells for high-power medium-voltage multilevel converters, *Proceedings of the IEEE Energy Conversion Congress and Exposition ECCE*, (2013), USA.

[14] Adamowicz M., Pietryka J., Giziewski S., Rutkowski M., Krzemiński Z., Układy sterowania bramkowego tranzystorów z węglika krzemu SiC JFET w falownikach napięcia, Przegląd Elektrotechniczny, R. 88, Nr 4b, (2012), 1-6.
[15] Ben Yaakov S., The benefits of planar magnetics in HF power conversion, *Source: http://www.paytongroup.com*
[16] Metallized Polypropylene (PP) Capacitors, *Source: http://www.wima.com/EN/mkp4.htm*
[17] Jin Li, Zheng Chen, Zhiyu Shen, Paolo Mattavelli, Jinjun Liu, Dushan Boroyevich, An adaptive dead-time control scheme for high-switching-frequency dual-active-bridge converter, Proc. Annual IEEE Applied Power Electronics Conference and Exposition (APEC), 2012, 1355 – 1361.
[18] Jun Huang, Yue Wang, Yuan Gao, Wanjun Lei, Ning Li, Modified Unified PWM Control to Operate the Dual Active Bridge Converters Under ZVS In the Whole Load Range, IEEE Conference Congress ECCE 2013, 620 – 625.
[19] Shenghui Cui, Dawei He, Mingxuan Li, Haifeng Lu, Thomas G.Habetler, Design of A Dual Half Bridge DC-DC Converter for An Ultra-capacitor based Auxiliary Power Source in Electric Vehicles, Proc. IEEE Transportation Electrification Conference and Expo (ITEC), 2012, 1-7.
[20] Stadler A., Gulden C., Improved thermal design of a high frequency power transformer, European Conf. on Power Electronics and Applications EPE 2011, s. 1–9.

***Authors**: dr inż. Marek Adamowicz; Politechnika Gdańska, Wydział Elektrotechniki i Automatyki, Katedra Automatyki Napędu Elektrycznego, ul. Sobieskiego 7, 80-216 Gdańsk, e-mail: madamowi@ely.pg.gda.pl; mgr inż. Patryk Strankowski, Politechnika Gdańska, Wydział Elektrotechniki i Automatyki, Katedra Automatyki Napędu Elektrycznego, ul. Sobieskiego 7, 80-216 Gdańsk, e-mail: strankowski@ely.pg.gda.pl; mgr inż. Jędrzej Pietryka, MMB Drives Sp. z o. o, ul. Sobieskiego 7, 80-216 Gdańsk, j.pietryka@mmb-drives.com.pl; mgr inż. Janusz Szewczyk, MMB Drives Sp. z o. o, ul. Sobieskiego 7, 80-216 Gdańsk, j.szewczyk@mmb-drives.com.pl; dr hab. inż. Jarosław Guziński, Politechnika Gdańska, Wydział Elektrotechniki i Automatyki, Katedra Automatyki Napędu Elektrycznego, ul. Sobieskiego 7, 80-216 Gdańsk, e-mail: jarguz@pg.gda.pl;*